DENTAL MATERIALS 35 (2019) 176–184

Available online at www.sciencedirect.com

ScienceDirect

journal homepage: www.intl.elsevierhealth.com/journals/dema

Novel *in vitro* comparative model of osteogenic and inflammatory cell response to dental implants

*Kelly M. Hotchkiss, Kegan T. Sowers, Rene Olivares-Navarrete**

Department of Biomedical Engineering, School of Engineering, Virginia Commonwealth University, Richmond, VA, USA

ARTICLE INFO

Article history:
Received 5 March 2018
Received in revised form
14 October 2018
Accepted 13 November 2018

Keywords:
Surface properties
Surface roughness
Surface chemistry
Inflammation
Biomaterials
Macrophages
Stem cells
Integration

ABSTRACT

Objectives. Roughened dental implants promote mesenchymal stem cell (MSCs) osteoblastic differentiation, and hydrophilic modifications induce anti-inflammatory macrophages activation. While the effect of different surface modifications on osseointegration of commercial dental implants have been compared *in vivo* and clinically, the initial cellular response to these modifications often overlooked. We aimed to characterize the macrophage inflammatory response and MSC osteogenesis across different commercially available implants *in vitro*.

Methods. Six commercially available rough implants [OsseoSpeed™ (Astra-Tech™, Implant A); Osseotite® (Biomet 3i™, Implant B); TiUnite™ (Nobel-Biocare®, Implant C); Ti-SLA®, (Implant D), Roxolid® (RXD-SLA, Implant E), RXD-SLActive® (Implant F) (Straumann®)] were examined. Macrophages and MSCs were seeded directly on implants and cultured in custom vials. mRNA and protein levels of pro- (IL1B, IL6, IL17A, CXCL10, TNFa) and anti- (IL4, IL10, TGFB1) inflammatory markers were measured after 24 and 48 h in macrophages. Osteoblastic differentiation of MSCs was assessed after seven days by alkaline phosphatase activity, osteocalcin, and angiogenic, osteogenic, and inflammatory markers by ELISA and qPCR ($n = 6$/variable, ANOVA, post hoc Tukey HSD with $\alpha = 0.05$).

Results. Hydrophilic implant F induced the highest level of osteogenic factor released from MSCs and anti-inflammatory factors from macrophages with the lowest level of pro-inflammatory factors. Alternatively, implants A and C supported lower levels of osteogenesis and increased secretion of pro-inflammatory factors.

Significance. In this study, we successfully evaluated differences in cell response to commercially available clinical implants using an *in vitro* model. Data from this model suggest that not all surface modification procedures generate the same cell response.

1. Introduction

Dental implants offer a reliable treatment for single tooth gaps in edentulous in patients [1] with high success rates and the potential to use smaller diameter implants or additional modifications to improve success [2] in difficult cases. The failures seen in early materials like gold, aluminum and porcelain lead to the introduction of biologically "inert" materials like titanium (Ti) and Ti alloys that were thought to not alter

* *Corresponding author at:* VCU School of Engineering, Department of Biomedical Engineering, 401 W. Main Street, Suite 1252, Richmond, VA 23284, USA.
E-mail address: ronavarrete@vcu.edu (R. Olivares-Navarrete).

https://doi.org/10.1016/j.dental.2018.11.011

the healing response after placement [3]. However, the original characterization of Ti as an inert material has evolved, with recent studies demonstrating that changes to Ti surface properties play an active role in controlling cell response [4–8]. Various surface modifications have been applied to clinical implants using both subtractive and additive methods including sandblasting, acid etching, anodization, and surface coatings. Rough implants increased bone-to-implant contact and overall clinical success [9,10] with faster healing rates and the potential for earlier loading times [1,11,12]. These results led to the development of different techniques to increase surface roughness on smooth dental implants. However, each procedure generates a roughened surface with slightly different topographical characteristics even when the arithmetic mean roughness is the same. Furthermore, the chemical and wettability characteristics of the material will also be altered as result of surface modifications and can drastically change the initial cell response to an implanted material.

Implant placement generates an immune response both to the injury and the material placed at the surgical site [13], with events during the first 24-h being critical to implant success. Cells of the innate immune system migrate to the site to clear debris and respond to the material. Macrophages are the primary effector cells that determine whether the response will be resolved quickly or prolonged. Therefore, materials modulating macrophage activation can enhance implant success. Macrophages can be activated to a pro-inflammatory phenotype and release factors (IL-1β, IL6, IL-12, IL17A, TNFα) that propagate the immune response or an anti-inflammatory phenotype to abrogate the immune response through cytokine release (IL-4 and IL-10) [14]. Once the immune response has been resolved, new bone tissue can begin to form. Bone formation can be generated by osteoblasts that differentiate from mesenchymal stem cells (MSCs) in contact with the implant surface.

One limit to testing implant surfaces in the past has been the use of replica surfaces created on 2D samples that model the surface presented on the clinically used implant. Since these are not the exact device used clinically, small differences may exist between the cell culture response and the *in vivo* results. Therefore, the purpose of our study was to create a rapid *in vitro* screening model for surface characteristics using inflammatory response and osteoblastic differentiation as read-outs using full-size, commercially available clinical dental implants.

2. Materials and methods

2.1. Implants

Five rough, hydrophobic, clinically used Ti or Ti-zirconium dental implants were used in this study: OsseoSpeed™ (AstraTech™ [implant A]); Osseotite® (Biomet 3i™ [implant B]); TiUnite™ (Nobel-Biocare® [implant C]); SLA® [implant D] and Roxolid® (RXD, TiZr alloy with 15 wt% Zr) SLA® [implant E] (Institut Straumann AG®). These hydrophobic implants were compared to rough hydrophilic RXD-SLActive® [implant F] (Straumann).

2.2. Material characterization

Surface roughness was quantified by scanning electron microscopy (SEM, Zeiss Auriga, Carl Zeiss, Jena, Germany) with 5 kV and ~2 mm working distance. Macroscale differences were assessed at 500× magnification while higher magnifications (5kx and 50kx) were used to compare micro- and nano-topographies. Quantitative surface roughness measurements were performed using laser scanning confocal microscopy (LSCM, Zeiss LSM 710, Carl Zeiss). Z-stacks were acquired with a focus area of 106.27 μm × 106.27 μm with a 20× objective, including thread edges and troughs. Average surface roughness was quantified with a 100 μm threshold at six different areas of three separate implants from each group.

Oxide layer composition was determined by X-ray photoelectron spectroscopy (XPS, ESCALAB 250, Thermo Scientific, Waltham MA) under ultra-high vacuum (10^{-9} Torr or below) with microfocused monochromatic AlKa X-ray source. Survey scans were completed at three points on each implant followed by high-resolution scans for carbon C1s, titanium Ti2p, oxygen O1s, sodium Na1s, chloride Cl2p, and zirconium Zr3d. ThermoAdvantage software (TA Instruments, New Castle, DE, USA) was used to assess spectrum results. Three areas were selected on separate implants for each group.

Surface wettability was determined by sessile drop contact angle (ramé-hart contact angle goniometer 250, model 100–25a, ramé-hart instrument co., Succasunna, NJ). 0.5 μL of deionized water was dropped on the unthreaded neck of each implant and imaged to determine the contact angle, with 0° representing hydrophilic, and angles greater than 80° representing hydrophobic surfaces.

2.3. Cell culture

Primary murine macrophages were differentiated from bone-marrow of 10–12 week old male C57Bl/6 mice (The Jackson Laboratory, Bar Harbor, ME) in accordance with the Institutional Animal Care and Use Committee (protocol AD10001108). Bones were removed, flushed with PBS, and plated at a density of 500,000 cells/mL after red cell lysis (ACK Buffer, ThermoFisher, Carlsbad, CA). Naïve macrophages were generated in culture in RPMI 1640 (ThermoFisher) supplemented with 10% fetal bovine serum (ThermoFisher), 50 U/mL penicillin-50 μg/mL streptomycin (ThermoFisher), 50 U/mL sodium pyruvate (ThermoFisher), and 30 ng/mL macrophage colony stimulating factor (M-CSF, PeproTech, Rocky Hill, NJ). After seven days, macrophages were subpassaged using non-enzymatic methods (Accutase, ThermoFisher) for experiments. Macrophages generated by this protocol [5,15,16] have been characterized as ≥80% positive for two macrophage specific markers CD68 + CD11b +. Human bone-marrow-derived MSCs (Lonza Biosciences, Walkersville, MD) were cultured in MSC Growth Medium (Lonza Biosciences). MSCs were sub passaged at 80% confluence and passage 3 cells used for experiments.

2.4. Cell plating

Macrophages (200,000 cells/cm^2) and MSCs (40,000 cells/cm^2) were plated directly onto the implant surface (~1.85 cm^2) in

50 μL media droplets to ensure direct interaction with the surface. Droplets were spread out over the implant surface to increase distribute cells evenly and avoid medium dripping. Implants were incubated at 37 °C for 2 h to facilitate cell attachment before implants were placed into custom culture vials containing 2 mL of media to fully submerge the implant for culture time points. Cells were cultured at 37 °C, 5% CO_2, and 100% humidity. The medium was exchanged every 48 h for MSC culture.

2.5. Cell staining

Cells were plated at 25% density to allow morphology to be observed on the surface. Cells were fixed for 30 min in PBS containing 4% paraformaldehyde. Cell membranes were permeabilized with 0.1% Triton X-100 (Sigma-Aldrich) and cytoskeleton stained with Alexa Fluor 488 conjugated phalloidin (0.165 μM) in PBS and nuclei stained using 2.5 ng/mL of Hoechst 34580 (ThermoFisher). Cells were imaged at three randomly selected regions on six separate implants using LSCM at 40 × magnification.

2.6. Gene expression

After one (macrophage) or seven days (MSCs) of culture, RNA was extracted using TriZOL (ThermoFisher) then quantified and 1 μg converted into cDNA. Custom Bio-Rad PCR arrays (Bio-Rad, Hercules, CA) were designed for inflammation and osteogenic differentiation. Inflammatory genes were measured in murine macrophages (*Ifng, Il1b, Il6, Il17a, Tnf, Il4, Il13, Il1rn, Tgfb1, Tgfb2, Tgfb3*) and MSCs (*TGFB1*). Levels of osteogenic markers (*RUNX2, ALPL, SP7, BGLAP, OPG, RANKL*), angiogenic markers (BMP2, TGFB1, VEGFA, FGF2), and inflammatory factors were measured in MSCs. Three housekeeping genes [glyceraldehyde 3-phosphate dehydrogenase (GAPDH), ribosomal protein S18 (RPS18), TATA-binding protein (TBP)] were used to normalize data.

2.7. Protein analysis

Secreted pro-inflammatory (TNFα, IL-1β, IL-6, IL-12, IL-17A [PeproTech, Rocky Hill, NJ] and IL-8 [R&D Systems, Minneapolis, MN]), anti-inflammatory (IL-4, IL-10 [PeproTech]), and osteogenic proteins (osteocalcin and osteoprotegerin [R&D Systems] RANKL, VEGFA, BMP-2 [PeproTech]) were quantified by ELISA. All secreted protein levels were normalized to DNA content using a Quant-iT^{TM} PicoGreen dsDNA Assay Kit (ThermoFisher) through the method described in the manufacturer's protocol. Alkaline phosphatase specific activity (ALP) was quantified in the cell lysates and normalized to total protein levels quantified through Macro BCA total protein assay (Sigma) as previously described [8].

2.8. Statistical analysis

Experiments were conducted with an n of six implants each. Macrophage experiments were conducted with primary cells pooled from eight donors. Experiments were performed three times and data presented are representative of one independent experiment. RNA expression was analyzed using ΔΔCT method normalized with housekeeping genes (GAPDH, RSP18, TBP) and TCPS. Prism GraphPad V7 software was used to analyze results. Data were found to be normally distributed based on analysis of QQ plots for each group. A one-factor, equal-variance analysis of variance (ANOVA) was used to test the null hypothesis that the group means were equal, against an alternative hypothesis that at least two of the group means were different, at an $\alpha = 0.05$ significance level. Once the p-value resulting from the initial ANOVA model was determined less than 0.05, multiple comparisons were made between group means with TUKEY-HSD. All experiments were repeated three times to validate results.

3. Results

3.1. Implant characterization

At 500 × and 5k× magnification each implant appeared visibly rough with differences in surface morphology between them (Fig. 1A). Microstructures on Implant C appeared as rounded pits while all others show a sharp peak morphology. At higher magnification (50kx) nanoscale differences were apparent, with nanostructures visible on implants F, A, B, and C but not on implants D and E. Quantitative average roughness (Fig. 1B) varied significantly, with higher values seen on implants A ($S_a = 3.12$ μm), B ($S_a = 3.11$ μm), and D ($S_a = 2.92$ μm) in comparison to implants C ($S_a = 1.29$ μm), E ($S_a = 2.26$ μm) and F ($S_a = 2.29$ μm). Contact angle analysis (Fig. 1C) demonstrated that A (112°), B (103°), C (100°), D (94°), and E (106°) were hydrophobic (contact angle (θ) >80°), while implant F was hydrophilic ($\theta = 0°$). XPS indicated clear differences in oxide layer composition (Fig. 1D). Carbon content varied considerably between each of the implant groups, with implant B (71% carbon) containing the highest levels.

3.2. Cell attachment

Both macrophages and MSCs were attached to the implant surface after two or four days of culture, respectively. DNA quantification following cell culturing showed little variance in DNA content of macrophages (Fig. 2A) and MSCs (Fig. 2B) on the implant surface between the groups.

3.3. Global changes in gene expression

Global gene expression analysis is shown in Fig. 3A. Vertical lines depict a 2-fold threshold in change, while the horizontal line indicates $p < 0.05$. Implant F showed the most significant upregulation of measured genes, while implants D and E upregulated slightly fewer genes. Implant B upregulated a similar number of genes as D and E, but with only moderate fold changes. Implants A and C showed an even distribution of up and down regulated genes and downregulated more genes than the other groups.

3.4. Immune response to clinical implants

Different implant surfaces facilitated changes in inflammatory genes in both macrophages (Fig. 3B) and MSCs (Fig. 3C).

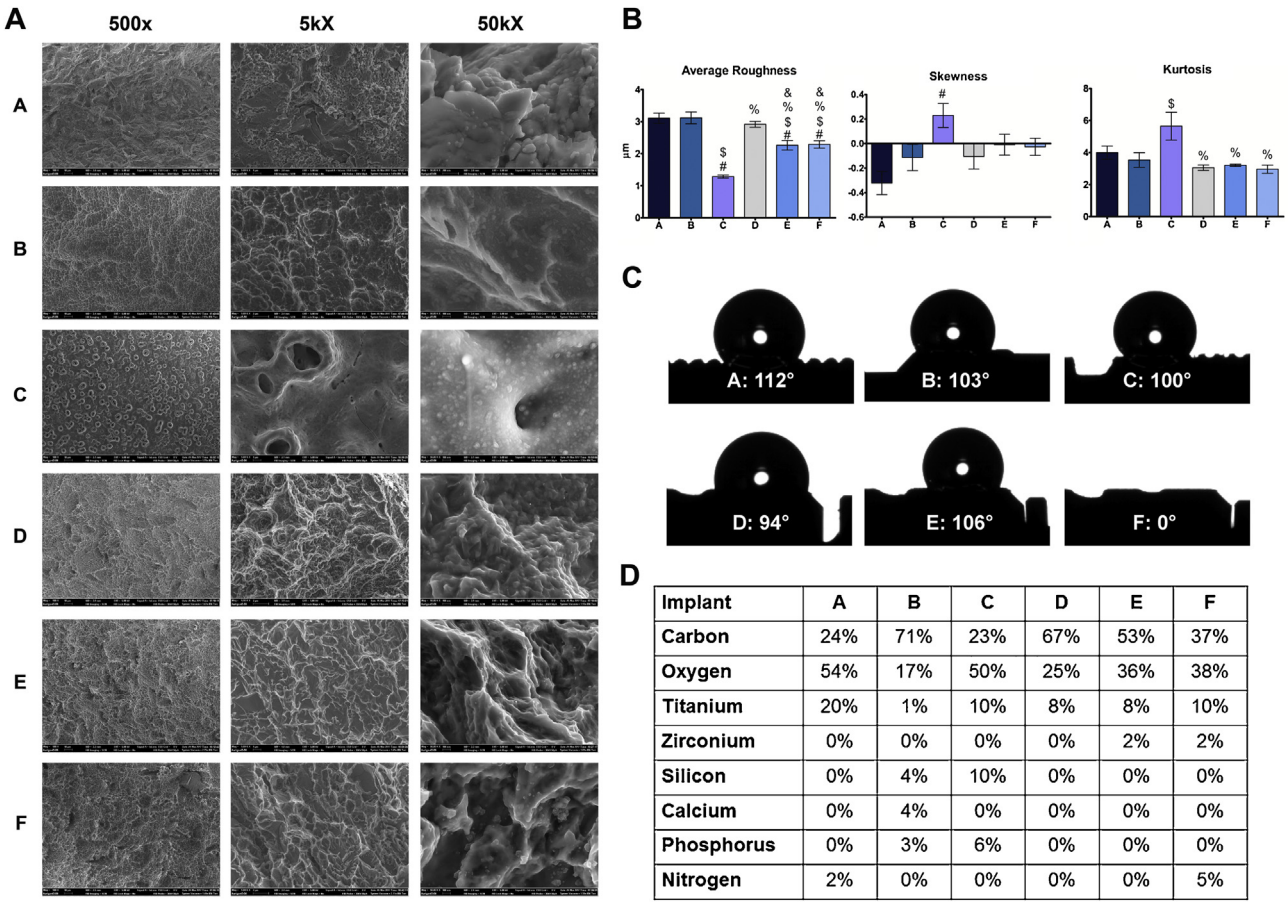

D

Implant	A	B	C	D	E	F
Carbon	24%	71%	23%	67%	53%	37%
Oxygen	54%	17%	50%	25%	36%	38%
Titanium	20%	1%	10%	8%	8%	10%
Zirconium	0%	0%	0%	0%	2%	2%
Silicon	0%	4%	10%	0%	0%	0%
Calcium	0%	4%	0%	0%	0%	0%
Phosphorus	0%	3%	6%	0%	0%	0%
Nitrogen	2%	0%	0%	0%	0%	5%

Fig. 1 – Comparison on implant surface characteristics. A. Qualitative SEM analysis at 500×, 5k×, and 50k×. B. Quantification of surface roughness by LSCM z-stack analysis. # $p < 0.05$ *vs.* implant A, $ *vs.* implant B, % *vs.* implant C, & *vs.* implant D. C. Contact angle assessment of surface wettability. D. XPS analysis of implant oxide layer composition.

After 24 h, macrophages on implants A and C upregulated pro-inflammatory mRNA (*Tnf, Il17a, Il1b, Infg*) while cells on E and F exhibited reduced expression (Fig. 3B). Expression of anti-inflammatory markers (*Il4, Il13, and Il1rn*) was significantly upregulated on implants E and F compared to A, B, C and D. *Tgfb1*, *Tgfb2* and *Tgfb3* were also upregulated on implants E and F. Likewise, macrophages cultured on implant A and C secreted the highest levels of pro-inflammatory proteins (TNFα, IL-17A, IL-1β, IL-12, IL-6) compared to other implants after 48 h (Fig. 4). The lowest levels of pro-inflammatory factors were released from cells on implants E and F. Implants E and F also promoted increased secretion of anti-inflammatory cytokines IL-4 and IL-10 by macrophages, with cells on implant F releasing the most.

Similarly, MSCs cultured for seven days on implants A and C released higher levels of pro-inflammatory IL-6 and IL-8, while cells on E and F released lower levels compared to control. E and F implants also promoted anti-inflammatory factor production with significant increases in IL-10 compared to other implants (Figs. 3C, 5).

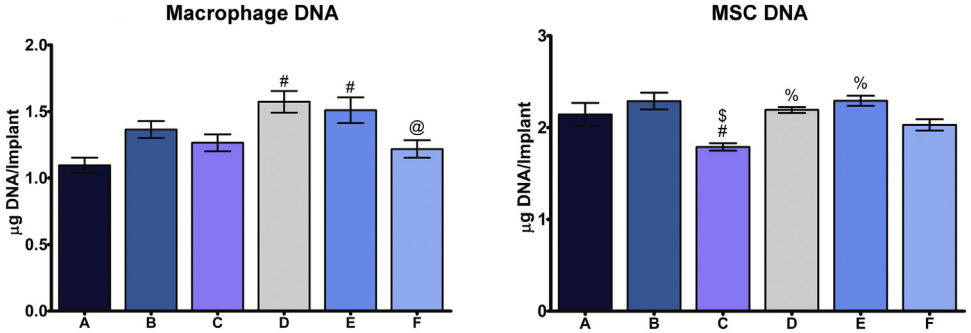

Fig. 2 – DNA quantification of macrophages and MSCs on each implant. # $p < 0.05$ *vs.* implant A, $ *vs.* implant B, % *vs.* implant C, & *vs.* implant D, @ *vs.* implant E.

3.5. *Osteogenic differentiation*

After seven days, MSCs on implants D, E, and F upregulated osteogenic associated genes, RUNX2, SP7 and BGLAP, while MSCs on A and C did not (Fig. 3C). Similarly, implants D, E, and F also upregulated BMP2, TGFB1, and VEGFA, genes associated with angiogenesis and bone induction. Additionally, MSCs on implant F produced the highest levels of ALP, an early marker of osteoblastic differentiation. Cells on implants A and C secreted lower levels of osteocalcin, a late-stage marker of osteogenic differentiation, than those on other implants, which all released similar levels. Cells on implant F produced the highest levels of BMP2 and VEGFA, suggesting a microenvironment that promotes strengthened osseointegration in comparison to other groups. Changes in markers of bone formation versus bone resorption were also evident between different implants in both RNA expression and protein secretion. Implant F increased production of OPG while simultaneously reducing levels of RANKL, which favors bone formation. In contrast, cells on implants A and C increased RANKL and reduced OPG, favoring bone resorption.

4. Discussion

Dental implants are highly successful in healthy patients, but further innovations are needed to improve performance in compromised patients. This study is of the first to establish a simple *in vitro* screening method to compare cell response across commercially available dental implants. While many

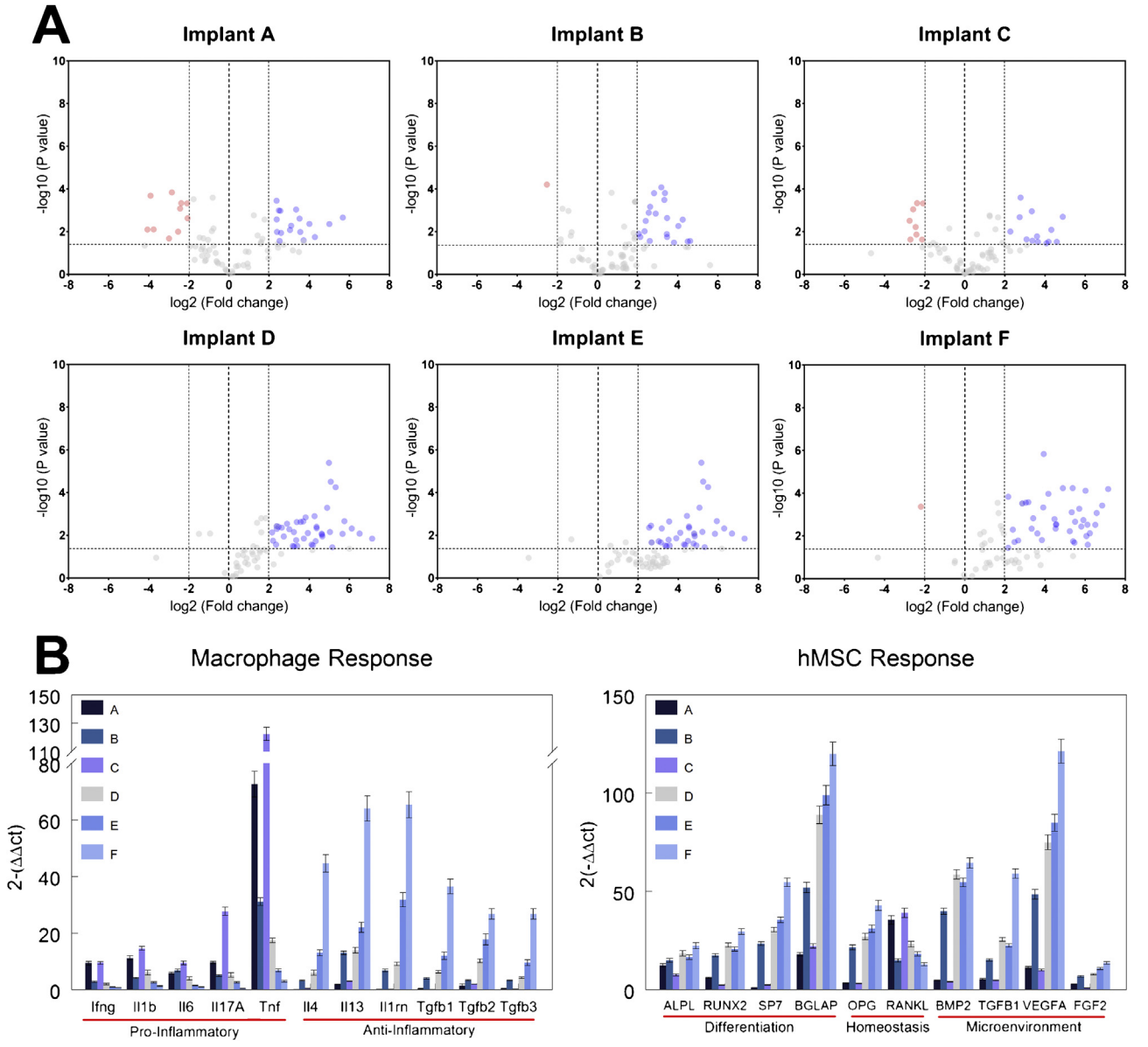

Fig. 3 – Gene expression changes in macrophages and MSCs. A. Volcano plots demonstrating global gene expression changes across both cell types. Significant upregulation shown (greater than 2-fold change) shown in purple, downregulation (less than −2-fold change) shown in red. B. Changes in inflammatory genes in macrophages and markers of osteoblastic differentiation and microenvironment production in MSCs. Implants groups from left to right (A, B, C, D, E, F) in bar graph.

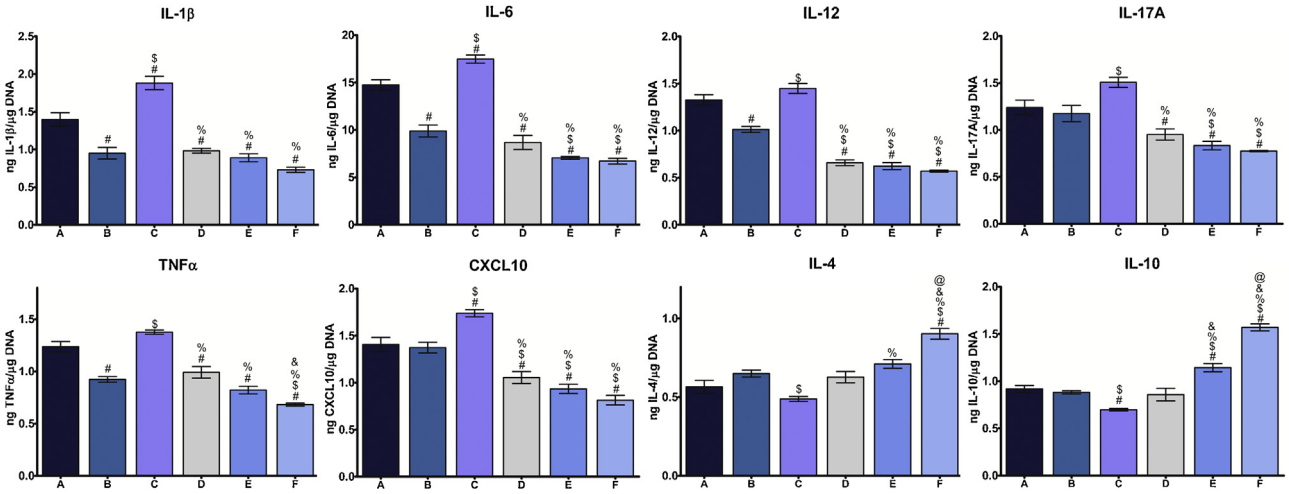

Fig. 4 – Inflammatory protein secretion from macrophages cultured on implants for 48 h. # $p < 0.05$ *vs.* implant A, $ *vs.* implant B, % vs. implant C, & *vs.* implant D, @ *vs.* implant E.

dental implant studies have looked at long-term osseointegration as implant success, generally after weeks or months following implantation, here we show the effects of surface modifications to clinical implants by initial inflammatory microenvironment production and osteoblastic differentiation. Although this study provides evidence of the cellular response to clinically used dental implants *in vitro* that can be correlated to *in vivo* and clinical studies published elsewhere, there are limitations due to the *in vitro* nature of this work. However, this study established an *in vitro* system that can rapidly screen clinically used dental implants using inflammatory response and cellular differentiation as readouts.

Advancements in dental implants have been achieved in large part through physical or chemical alteration on the implant surface. The most common modifications to surface topography are created by roughening the surface of the implant physically (*e.g.*, sandblasting) or chemically (*e.g.*, acid etching) [10,17]. Additionally, modifications to increase corrosion resistance (*e.g.*, anodization) [11], modify surface energy or vary the surface composition by adding different elements [8,18] have been developed. While many surface modifications have been proposed to increase osseointegration and the overarching goal of greater implant success [17,19], only a handful of modifications have successfully been translated into the clinic. Several studies have characterized successful modification to surface roughness, oxide layer composition, and wettability of clinically relevant dental implants [12,20]. Results from these studies, while fundamental from the material characteristics perspective, are unable to predict biological outcomes and rely heavily on studies carried on 2D replicas with similar modifications [21]. The basic understanding of the effects of dental implant surface characteristics has been generated in samples that are processed with similar protocols as clinical implants, but differences in surface parameters are evident across publications [19,21,22].

Our results showed that among the implants tested, C had the lowest average surface roughness, possibly due to the unique morphology and wide spacing of microstructures. The pocket-like pits on this surface could be used to store therapeutic agents or retain contamination, which both may play a role in ultimate osseointegration. This potentially negative outcome from morphology may be correlated to bone loss seen surrounding these implants in clinical retrospective studies after 5 years [23]. Each of the other implants displayed

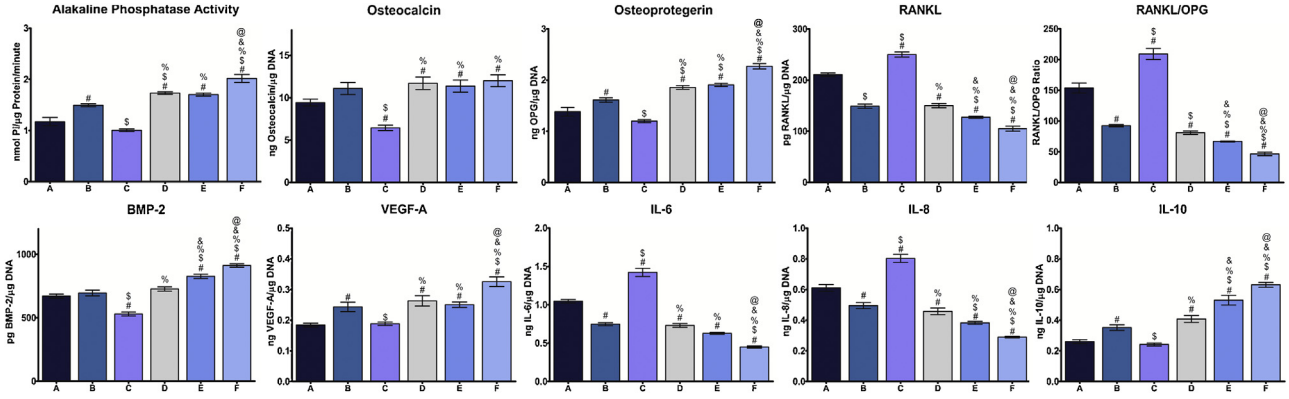

Fig. 5 – Osteogenic and inflammatory protein secretion from MSCs cultured on implants for 48 h. # $p < 0.05$ *vs.* implant A, $ *vs.* implant B, % *vs.* implant C, & *vs.* implant D, @ *vs.* implant E.

a sharp peak morphology more similar to bone resorption following osteoclast activation [24]. This change in performance suggests how implant surface topography can alter cell response both initially and overtime. In addition to generating bio-mimicking morphologies, some companies have begun "doping" the implant surface with elements in an effort to promote bone formation. This was seen in the elevated fluoride levels measured in implant A. Implants E and F, the only two TiZr alloy implants, were found to have the next lowest S_a values. The lower roughness of these two implants compared to pure Ti A, B and D implants may be due to the harder material responding differently to mechanical roughness modifications. The roughness values measured in this study range from 1.2 μm to 3.29 μm, which is higher than values quantified by reviews comparing surface properties of commercially available implants [25]. As a standard operating procedure for quantifying surface roughness on cylindrical implants has not been established, these differences can be attributed to the selection of difference scan sizes, cutoff thresholds, or the use of filters on each machine.

In general, all the implants allowed similar levels of cell attachment and similar levels of DNA content after 7 days, indicating that changes in surface topography, chemistry, and energy did not substantially affect cellular attachment and proliferation. However, differences were found in macrophage and MSC gene expression on each implant. Implants A and C significantly increased expression of pro-inflammatory genes and reduced expression of anti-inflammatory genes, while Implant F decreased expression of pro-inflammatory and increased expression of anti-inflammatory genes. Changes in gene expression were matched in protein release. These results confirm previous reports by our group and others indicating that hydrophilic surfaces preferentially activate macrophages into an anti-inflammatory phenotype that can result in faster healing and osseointegration [5]. We believe that the changes in surface wettability may induce differential protein adsorption and subsequent cell interaction. While each hydrophobic surface was found to have similar contact angle and therefore assumed to have similar wettability, there were differences in oxide layer composition. Both implants A and C displayed a higher percent of oxygen and lower carbon compared to others, which interestingly did not increase wettability in our model. The change in oxide layer can control the protein adsorption exposing different epitopes to influence cell activation toward a potential pro-inflammatory phenotype. Previous studies have correlated expression of pro-inflammatory TNFα with clinical complications at early stages [26], suggesting a surface able to control the inflammation is desired. In addition to decreasing the pro-inflammatory microenvironment, a faster resolution of the initial inflammation can also improve success. IL-10 is a classical immunomodulatory cytokine, and our results showed that hydrophilicity plays a fundamental role in increased expression and release of this cytokine.

Once the inflammatory response has subsided, progenitor cells or MSCs will migrate to the implant and start the de novo bone formation [27]. Several studies from our lab and others have shown that surface roughness and topography promote osteoblastic differentiation, in Ti 2D samples, traditionally measured by an increase in ALP and osteocalcin levels [28,29]. We found all implant surfaces promote ALP and osteocalcin, suggesting that all implants could successfully osseointegrate. While our results are similar to those found by other groups comparing one or two of the selected implant surfaces, differences can arise due to culture times and sterilization techniques. Groups who chose to UV sterilize disks [30] prior to use may modify protein adsorption and subsequent cell response by generating a more hydrophilic surface that was originally present. In this study, we used gamma-irradiated implants packaged and sent directly from manufacturer without further sterilization techniques. Increased levels of osteoblast differentiation markers were also measures on surface replicas from stem cells cultured for as few as 3 days [30] and up to 7 days [7] as with this study. However, significant differences were present in the amount of activity and protein release. This indicates that while each surface had similar global roughness values, the cells could discriminate between topographical parameters on the surfaces. In this respect, cells grown in Implant C showed the lowest levels of ALP and osteocalcin. This implant also showed the lowest average roughness and the only with a positive skewness and the highest kurtosis. Higher levels of osteoblastic differentiation markers measured on Implants E and F correspond to faster healing, osseointegration and loading times seen in clinical and preclinical animal studies [31,32]. This study shows that not all roughness is considered the same when considering differentiation or pro-bone forming microenvironment production. While Implants D, E, and F generated higher OPG to RANKL ratios, supporting bone formation over resorption, Implant A and Implant C promoted more RANKL release and less OPG [33]. The higher levels of RANKL could be attributed to changes in surface morphology or to surface chemistry. Studies have found that higher levels of fluoride can have detrimental effects on bone forming cells [34] leading to disruption in bone homeostasis. The elevated level of fluoride present in the oxide layer of Implant A may promote the release of osteoclast activating RANKL and would be interesting to study further. This switch to higher osteoclast forming RANKL production may favor bone resorption and remodeling. Additionally, we found that MSCs produced the highest levels of IL-6 and IL-8 in Implant C, with the lowest levels of IL-10, indicating a pro-inflammatory microenvironment. While hydrophilic implant F favored an anti-inflammatory microenvironment. While investigating the mechanisms by which some dental implants produce a more pro-inflammatory environment were out of the scope of this work, we can speculate that the physicochemical changes observed in implant C and, in some magnitude, implant A can affect the interaction between the implant surface and the proteins present in the medium, resulting in a preferential protein adsorption or changes in the motifs presented for cell recognition. Several studies have shown that changes in surface chemistry and surface topography affect protein adsorption, including proteins that can affect the immune response [35–37]. Moreover, these physicochemical changes can produce changes in cellular behavior [35,36].

Overall, this study showed that clinical implants could be used as a rapid screening tool to help predict how newly developed surface modifications may affect biological outcome.

While all the implants promoted osteoblastic differentiation, the differences in surface characteristics create different cellular responses that can be detected by a simple *in vitro* set up. These differences in protein release and microenvironment suggest differences in healing and osseointegration times that may alter the outcome of the treatment.

Author contributions

KMH and RON design study, planned experiments, analyzed and interpreted data. KMH and KTS conducted implant characterization and biological experiments. KMH, KTS, and RON prepared manuscript.

Acknowledgements

The authors would like to thank Institut Straumann AG for providing the six different implants compared in this study.

REFERENCES

[1] Esposito M, Grusovin MG, Willings M, Coulthard P, Worthington HV. The effectiveness of immediate, early, and conventional loading of dental implants: a Cochrane systematic review of randomized controlled clinical trials. Int J Oral Maxillofac Implants 2007;22:893–904.
[2] Davarpanah M, Martinez H, Tecucianu JF, Celletti R, Lazzara R. Small-diameter implants: indications and contraindications. J Esthet Dent 2000;12:186–94.
[3] von Wilmowsky C, Moest T, Nkenke E, Stelzle F, Schlegel KA. Implants in bone: part I. A current overview about tissue response, surface modifications and future perspectives. Oral Maxillofac Surg 2014;18:243–57, http://dx.doi.org/10.1007/s10006-013-0398-1.
[4] Alfarsi MA, Hamlet SM, Ivanovski S. Titanium surface hydrophilicity modulates the human macrophage inflammatory cytokine response. J Biomed Mater Res A 2014;102:60–7, http://dx.doi.org/10.1002/jbm.a.34666.
[5] Hotchkiss KM, Reddy GB, Hyzy SL, Schwartz Z, Boyan BD, Olivares-Navarrete R. Titanium surface characteristics, including topography and wettability, alter macrophage activation. Acta Biomater 2016;31:425–34, http://dx.doi.org/10.1016/j.actbio.2015.12.003.
[6] Hyzy SL, Olivares-Navarrete R, Hutton DL, Tan C, Boyan BD, Schwartz Z. Microstructured titanium regulates interleukin production by osteoblasts, an effect modulated by exogenous BMP-2. Acta Biomater 2013;9:5821–9, http://dx.doi.org/10.1016/j.actbio.2012.10.030.
[7] Olivares-Navarrete R, Hyzy SL, Gittens RA, Schneider JM, Haithcock DA, Ullrich PF, et al. Rough titanium alloys regulate osteoblast production of angiogenic factors. Spine J 2013;13:1563–70, http://dx.doi.org/10.1016/j.spinee.2013.03.047.
[8] Zhao G, Schwartz Z, Wieland M, Rupp F, Geis-Gerstorfer J, Cochran DL, et al. High surface energy enhances cell response to titanium substrate microstructure. J Biomed Mater Res A 2005;74:49–58, http://dx.doi.org/10.1002/jbm.a.30320.
[9] Wennerberg A, Albrektsson Galli. Current knowledge about the hydrophilic and nanostructured SLActive surface. Clin Cosmet Investig Dent 2011;3:59–67, http://dx.doi.org/10.2147/CCIDE.S15949.
[10] Wennerberg A, Albrektsson T. Effects of titanium surface topography on bone integration: a systematic review. Clin Oral Implants Res 2009;20:172–84, http://dx.doi.org/10.1111/j.1600-0501.2009.01775.x.
[11] Ma Q-L, Zhao L-Z, Liu R-R, Jin B-Q, Song W, Wang Y, et al. Improved implant osseointegration of a nanostructured titanium surface via mediation of macrophage polarization. Biomaterials 2014;35:9853–67, http://dx.doi.org/10.1016/j.biomaterials.2014.08.025.
[12] Scharer P, Glauser R, Ruhstaller P, Windisch S, Zembic A, Lundgren A, et al. Immediate occlusal loading of branemark systemR TiUnite™ implants placed predominantly in soft bone: 4-year results of a prospective clinical study. Clin Implant Dent Relat Res 2005;7 s:52–9, http://dx.doi.org/10.1111/j.1708-8208.2005.tb00075.x.
[13] Franz S, Rammelt S, Scharnweber D, Simon JC. Immune responses to implants — a review of the implications for the design of immunomodulatory biomaterials. Biomaterials 2011;32:6692–709, http://dx.doi.org/10.1016/j.biomaterials.2011.05.078.
[14] Mantovani A, Biswas SK, Galdiero MR, Sica A, Locati M. Macrophage plasticity and polarization in tissue repair and remodelling. J Pathol 2013;229:176–85, http://dx.doi.org/10.1002/path.4133.
[15] Hotchkiss KM, Ayad NB, Hyzy SL, Boyan BD, Olivares-Navarrete R. Dental implant surface chemistry and energy alter macrophage activation in vitro. Clin Oral Implants Res 2016;28(4):414–23, http://dx.doi.org/10.1111/clr.12814.
[16] Hotchkiss KM, Clark NM, Olivares-Navarrete R. Macrophage response to hydrophilic biomaterials regulates MSC recruitment and T-helper cell populations. Biomaterials 2018;182:202–15, http://dx.doi.org/10.1016/J.BIOMATERIALS.2018.08.029.
[17] Le Guéhennec L, Soueidan A, Layrolle P, Amouriq Y. Surface treatments of titanium dental implants for rapid osseointegration. Dent Mater 2007;23:844–54, http://dx.doi.org/10.1016/j.dental.2006.06.025.
[18] Berglundh T, Abrahamsson I, Albouy J-P, Lindhe J. Bone healing at implants with a fluoride-modified surface: an experimental study in dogs. Clin Oral Implants Res 2007;18:147–52, http://dx.doi.org/10.1111/j.1600-0501.2006.01309.x.
[19] Smeets R, Stadlinger B, Schwarz F, Beck-Broichsitter B, Jung O, Precht C, et al. Impact of dental implant surface modifications on osseointegration. Biomed Res Int 2016;2016, http://dx.doi.org/10.1155/2016/6285620, 6285620.
[20] Roccuzzo M, Aglietta M, Bunino M, Bonino L. Early loading of sandblasted and acid-etched implants: a randomized-controlled double-blind split-mouth study. Five-year results. Clin Oral Implants Res 2008;19:148–52, http://dx.doi.org/10.1111/j.1600-0501.2007.01426.x.
[21] Jarmar T, Palmquist A, Brånemark R, Hermansson L, Engqvist H, Thomsen P. Characterization of the surface properties of commercially available dental implants using scanning electron microscopy focused ion beam, and high-resolution transmission electron microscopy. Clin Implant Dent Relat Res 2008;10:11–22, http://dx.doi.org/10.1111/j.1708-8208.2007.00056.x.
[22] Rupp F, Liang L, Geis-Gerstorfer J, Scheideler L, Hüttig F. Article in press Surface characteristics of dental implants: a review. Dent Mater 2017;34(1):40–57, http://dx.doi.org/10.1016/j.dental.2017.09.007.
[23] Pettersson P, Sennerby L. A 5-year retrospective study on replace select tapered dental implants. Clin Implant Dent Relat Res 2015;17:286–95, http://dx.doi.org/10.1111/cid.12105.

[24] Hefti T, Frischherz M, Spencer ND, Hall H, Schlottig F. A comparison of osteoclast resorption pits on bone with titanium and zirconia surfaces. Biomaterials 2010;31:7321–31, http://dx.doi.org/10.1016/j.biomaterials.2010.06.009.
[25] Wennerberg A, Albrektsson T. On implant surfaces: a review of current knowledge and opinions. Int J Oral Maxillofac Implants 2009;24:63–74.
[26] Slotte C, Lennerås M, Göthberg C, Suska F, Zoric N, Thomsen P, et al. Gene expression of inflammation and bone healing in peri-implant crevicular fluid after placement and loading of dental implants. A kinetic clinical pilot study using quantitative real-time PCR. Clin Implant Dent Relat Res 2012;14:723–36, http://dx.doi.org/10.1111/j.1708-8208.2010.00309.x.
[27] Davies JE. Understanding peri-implant endosseous healing. J Dent Educ 2003;67:932–49.
[28] Olivares-Navarrete R, Raines AL, Hyzy SL, Park JH, Hutton DL, Cochran DL, et al. Osteoblast maturation and new bone formation in response to titanium implant surface features are reduced with age. J Bone Miner Res 2012;27:1773–83, http://dx.doi.org/10.1002/jbmr.1628.
[29] Zhu X, Chen J, Scheideler L, Reichl R, Geis-Gerstorfer J. Effects of topography and composition of titanium surface oxides on osteoblast responses. Biomaterials 2004;25:4087–103, http://dx.doi.org/10.1016/j.biomaterials.2003.11.011.
[30] Masaki C, Schneider GB, Zaharias R, Seabold D, Stanford C. Effects of implant surface microtopography on osteoblast gene expression. Clin Oral Implants Res 2005;16:650–6, http://dx.doi.org/10.1111/j.1600-0501.2005.01170.x.
[31] Buser D, Schenk RK, Steinemann S, Fiorellini JP, Fox CH, Stich H. Influence of surface characteristics on bone integration of titanium implants. A histomorphometric study in miniature pigs. J Biomed Mater Res 1991;25:889–902, http://dx.doi.org/10.1002/jbm.820250708.
[32] Gottlow J, Dard M, Kjellson F, Obrecht M, Sennerby L. Evaluation of a new titanium-zirconium dental implant: a biomechanical and histological comparative study in the mini pig. Clin Implant Dent Relat Res 2012;14:538–45, http://dx.doi.org/10.1111/j.1708-8208.2010.00289.x.
[33] Han J, Chen Z, Li W, Meng H. [Determination of bone metabolic marker levels in perio-implant crevicular fluid and analysis of dental implants stability by resonance frequency in the early stage of healing]. Beijing Da Xue Xue Bao 2015;47:37–41.
[34] Everett ET. Fluoride's effects on the formation of teeth and bones, and the influence of genetics. J Dent Res 2011;90:552–60, http://dx.doi.org/10.1177/0022034510384626.
[35] Choi S-H, Jeong W-S, Cha J-Y, Lee J-H, Lee K-J, Yu H-S, et al. Effect of the ultraviolet light treatment and storage methods on the biological activity of a titanium implant surface. Dent Mater 2017;33:1426–35, http://dx.doi.org/10.1016/j.dental.2017.09.017.
[36] Araújo-Gomes N, Romero-Gavilán F, Sánchez-Pérez AM, Gurruchaga M, Azkargorta M, Elortza F, et al. Characterization of serum proteins attached to distinct sol-gel hybrid surfaces. J Biomed Mater Res Part B Appl Biomater 2017, http://dx.doi.org/10.1002/jbm.b.33954.
[37] Romero-Gavilán F, Gomes NC, Ródenas J, Sánchez A, Azkargorta M, Iloro I, et al. Proteome analysis of human serum proteins adsorbed onto different titanium surfaces used in dental implants. Biofouling 2017;33:98–111, http://dx.doi.org/10.1080/08927014.2016.1259414.